Determination of the Molecular Arrangement Inside Cyanine Dye Aggregates by Magnetic Orientation

I. O. Shklyarevskiy,*,† P. C. M. Christianen,† E. Aret,‡ H. Meekes,‡ E. Vlieg,‡ G. Deroover,§ P. Callant,§ L. van Meervelt,|| and J. C. Maan†

High Field Magnet Laboratory, NSRIM, University of Nijmegen, Toernooiveld 7, 6525 ED Nijmegen, The Netherlands, Department of Solid State Chemistry, NSRIM, University of Nijmegen, Toernooiveld 1, 6525 ED Nijmegen, The Netherlands, AGFA-Gevaert N. V., Septestraat 27, B-2640, Mortsel, Belgium, and Department of Chemistry, KULeuven, Celestijnenlaan 200F, B-3001, Leuven, Belgium

Received: January 6, 2004; In Final Form: August 2, 2004

We present a novel method for the determination of the internal structure of macromolecular aggregates in solution based on polarized absorption measurements on magnetically aligned aggregates. Different types of aggregates of three cyanine dyes were investigated in order to test the method. The obtained stacking geometries agree with those found by X-ray diffraction experiments on single crystals grown from the studied dyes, providing evidence that our method is a valuable tool for structural analysis of molecular assemblies.

I. Introduction

Molecular aggregates are formed by spontaneous self-assembly of molecules into ordered architectures, held together by noncovalent interactions. Generally, the specific molecular arrangement inside an aggregate is intimately related to the chemical structure of the molecule. In turn, the structure of the aggregate largely determines its physical properties. The relationship between molecular structure, type of aggregate, and resulting properties is, however, often difficult to predict, and the degree of ordering is not seldom far from perfect. Supramolecular chemistry aims to design and synthesize novel molecular building blocks that self-organize in well-defined, perfectly ordered architectures with tailor-made properties, often inspired by biological systems, such as DNA[1] and light-harvesting complexes of the natural photosynthetic system.[2] Recently, the interest in molecular aggregates has increased tremendously, after the notion that molecular self-assembly could play a major role in the bottom-up construction of nanoscale objects, such as wires[3,4] and rings,[5] as opposed to the top-down method currently employed for fabrication of semiconductor devices.

The ability to determine experimentally the stacking of molecules inside aggregates is therefore important in order to gain understanding of the relation between internal structure and physical properties, and to improve these for future application in real devices. Techniques regularly used for the determination of the internal structure of crystals (such as X-ray and neutron diffraction) often cannot be applied to aggregates because of their limited size or because they are destroyed by the probing beam. Alternatively, scanning probe techniques such as AFM,[6,7] STM,[8] and NSOM[9,10] only probe architectures at the surface of the substrate, where the internal structure can be different from the one in the solution in which aggregates are formed. Cryo-TEM was demonstrated to be very useful to determine the molecular structure,[11] although great care is required not to destroy the aggregates upon freezing. It would therefore be useful to measure the molecular order of aggregates in solution, their native environment. In this regard an intrinsic difficulty arises, namely that the Brownian motion of the aggregates hampers easy determination of almost any property, since it is averaged over many aggregates that are randomly oriented in space.

In this paper we present a new method, which overcomes this problem by measuring the anisotropic optical response of cyanine dye aggregates that are macroscopically oriented in high magnetic fields. We demonstrate that the internal molecular arrangement can be deduced from the polarized absorbance spectra of aligned aggregates in solution. To illustrate our method we have chosen to work with cyanine dye aggregates, but it should be emphasized that the method can also be applied to aggregates of other organic materials. Cyanine dyes feature very strong optical absorption, which leads to characteristic optical properties upon self-organization into supramolecular aggregates. For this reason cyanine aggregates are widely applied in silver halide photography,[12] photodynamic therapy for cancer,[13] and laser technology,[14] and are very promising for nonlinear optical devices[15,16] and for producing molecular fibers.[9] Various types of stacking geometries have been identified, ranging from simple one-dimensional arrangements, such as brickwork or ladder type of stacking, to more complicated types, such as herringbone stacking, or sometimes even fully three-dimensional arrangements.[17] Depending on the type of molecular ordering, the absorption spectrum shifts to the red (so-called J-aggregates,[18,19] e.g., brickwork) or to the blue (H-aggregates,[20] e.g., ladder), as compared to the spectrum of an isolated monomer. The spectral shift of the absorption peak is caused by the interactions between neighboring optical dipoles and depends strongly on the relative arrangement of adjacent chromophores, that is, on the relative orientation of the molecules.[21,22]

There are several reasons why we have chosen cyanine dyes as a model system for our investigations. First, the optical properties of the cyanine molecules are well-known and very

* Corresponding author. Telephone: +31-(0)24-3652237. Fax: +31-(0)24-3652440. E-mail: igors@sci.kun.nl.
† High Field Magnet Laboratory, University of Nijmegen.
‡ Department of Solid State Chemistry, University of Nijmegen.
§ AGFA-Gevaert N. V.
|| KULeuven.

10.1021/jp049945j CCC: $27.50
Published on Web 09/28/2004

anisotropic, and by measuring the anisotropy in absorption the orientation of the molecule in real space can be inferred. Second, by introducing small variations in the molecular structure, completely different aggregate structures can be obtained, which provides a good testing system for our method. Finally, it is possible to grow single crystals of the used dyes, of which the crystal structure can be determined by X-ray diffraction (XRD) experiments and in turn can be compared to the structure found by the field alignment method.

We report results obtained on three different cyanine dye molecules, each of them forming a different type of aggregate. The aggregate solutions were aligned in a high magnetic field, and the polarized absorption spectra were measured. From the optical anisotropy the internal structure of the aggregate was determined, which was found to be in good agreement with the crystal structure deduced from the X-ray diffraction on the single crystals and on powdered aggregate samples.

The paper is organized as follows. In section II the theory of magnetic field alignment of diamagnetic substances and its possible influence on the polarized absorption spectra are discussed. Experimental details of high magnetic field and X-ray experiments, together with the details of the preparation of the aggregate solution and single crystal growth, are presented in section III. Section IV describes the results of the magnetic field alignment and X-ray experiments, which are discussed extensively in section V. Conclusions and perspectives are outlined in section VI.

II. Theory

A. Magnetic Field Induced Orientation. Since most organic molecules are diamagnetic, magnetic fields provide a powerful tool to manipulate molecular matter. If a molecule is placed in a magnetic field, the intramolecular electronic screening currents generate a diamagnetic moment $\vec{m}$ proportional to the magnetic field $\vec{B}$:

$$\vec{m} = \boldsymbol{\chi}\vec{B} \tag{1}$$

where $\boldsymbol{\chi}$ is a second-rank symmetric tensor representing the diamagnetic susceptibility. This tensor can be diagonalized by choosing the proper coordinate system ($\chi_{ik} = 0$ for $i \neq k$). In most practical cases $\boldsymbol{\chi}$ can be approximated by an ellipsoid such that it possesses only two different diagonal components: $\chi_\perp$ along the short ellipsoidal axis and $\chi_{||}$ along the long ellipsoidal axis.

The magnetic moment $\vec{m}$ is interacting with the applied magnetic field and the molecule will acquire an extra energy:

$$E_{\mathrm{mag}} = -\frac{1}{\mu_0}\vec{m}\cdot\vec{B} \tag{2}$$

where μ_0 is the permeability of the free space.

Here we are only interested in the term that is anisotropic in the magnetic field:[23]

$$E_{\mathrm{mag}} = -\frac{1}{\mu_0}\Delta\chi B^2 \cos^2\theta \tag{3}$$

where $\Delta\chi = \chi_{||} - \chi_\perp$ is an anisotropy of diamagnetic susceptibility, and θ is the angle between the long molecular axis with and the magnetic field direction. This equation expresses the fact that the amount of extra energy in an applied magnetic field depends on the molecular orientation with respect to the field direction. This leads to an orientational force, tending to minimize the energy, toward an orientation with the axis of smallest diamagnetic susceptibility along the field. Precise determination of $\Delta\chi$ for a single molecule is difficult and ambiguous; thus we will further use the anisotropy in the molar diamagnetic susceptibility $\Delta\chi_{\mathrm{m}} = \Delta\chi N_{\mathrm{A}}$, where N_{A} is Avogadro's number. The textbook example[24] is a benzene molecule which has a large anisotropy $\Delta\chi_{\mathrm{m}} \approx -7.5 \times 10^{-10}$ m^3/mol (SI units) and tends to orient with the plane of the molecule parallel to the field direction, to avoid large induced currents in the ring that give rise to larger diamagnetic susceptibility and higher magnetic energy.

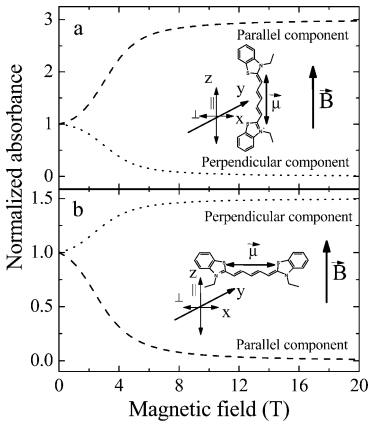

Figure 1. Evolution of normalized absorbance with molecular orientation parallel (a) and perpendicular (b) to magnetic field direction. The curves are calculated using $\Delta\chi_{\mathrm{m}} = 4.5 \times 10^{-9}$ m^3/mol and $N = 3 \times 10^5$ stacked molecules with their long axes in one direction.

As a result of thermal motion, the orientation of a molecule in a magnetic field is given by a distribution function $f(\theta,\phi)$ dΩ, the probability of finding the molecule in a small solid angle d$\Omega = \sin\theta\ \mathrm{d}\theta\ \mathrm{d}\phi$. The distribution function that is commonly used to describe the molecular orientation in a magnetic field is the Maxwell−Boltzmann distribution function:

$$f(\theta) \propto \exp\left(-\frac{\Delta\chi_{\mathrm{m}}B^2}{\mu_0 N_{\mathrm{A}} kT}\cos^2\theta\right) \tag{4}$$

(If the molecules orient perpendicular to the magnetic field direction, $\cos^2\theta$ should be replaced by $\sin^2\theta$.)

However, for individual molecules, the change in energy is small compared to the thermal energy ($\Delta\chi B^2 \ll kT$), and it is not possible to magnetically align single molecules at fields that are experimentally accessible nowadays. Magnetic field alignment is therefore only applicable to materials such as macromolecules (polymers), liquid crystals, or molecular aggregates, which contain a sufficient number of coupled or correlated molecules (N) to result in a magnetic torque that is large enough to induce appreciable orientational order ($N\Delta\chi B^2 \gg kT$). Recently we have shown that in the case of J-aggregates of cyanine dyes N indeed can be made sufficiently large ($N >$ 20 000) to achieve magnetic field induced alignment.[25]

B. Polarized Absorption. To determine the degree of alignment and to follow the orientation process, we take advantage of the well-defined anisotropic absorption properties of cyanine dyes. The optical transition dipole moment $\vec{\mu}$ of a cyanine dye molecule is parallel to the line connecting the nitrogen atoms (inset Figure 1). Consider a cyanine molecule of which the dipole moment makes an angle θ with the z-axis, the direction of the magnetic field, and an angle ϕ with the x-axis. The absorption of this molecule parallel ($A_{||}$) and perpendicular ($A_\perp$) to the magnetic field depends on the angle of $\vec{\mu}$ with the electric field vector $\vec{E}$ of the incident light beam,

$\vec{\mu}\cdot\vec{E}$. For light polarized parallel to the *z*-axis $\vec{\mu}\cdot\vec{E} = \mu E \cos\theta$, which leads to[26]

$$A_{\parallel} = A_0 \cos^2\theta \tag{5}$$

Similarly, light polarized perpendicular to the *z*-axis gives $\vec{\mu}\cdot\vec{E} = \mu E \sin\theta \cos\phi$, which results in

$$A_{\perp} = A_0 \sin^2\theta \cos^2\phi \tag{6}$$

In the case of an ensemble of molecules their orientation in a magnetic field is given by the orientation distribution function in eq 4. As a consequence, the measured absorbance of the solution, parallel and perpendicular to the magnetic field, yields

$$A_{\parallel} = A_0 \frac{\int f(\theta) \cos^2\theta \sin\theta \, d\theta}{\int f(\theta) \sin\theta \, d\theta} \tag{7}$$

$$A_{\perp} = A_0 \frac{\int\int f(\theta) \sin^3\theta \cos^2\varphi \, d\theta \, d\varphi}{\int\int f(\theta) \sin\theta \, d\theta \, d\varphi} \tag{8}$$

where A_0 denotes the absorbance at zero magnetic field, and the denominator corresponds to the normalization of the distribution function.

As described in the previous paragraph, an aromatic ring tends to align to a direction in which the plane of the ring is parallel to the field direction, which, at first sight, still leaves two possible alignment directions for cyanine dyes, with the long molecular axis parallel (Figure 1a) or perpendicular (Figure 1b) to the field. Figure 1 shows the normalized absorbance ($A_{\parallel}/A_0$ and $A_{\perp}/A_0$) for both cases, to illustrate the clear difference.

In the first case (Figure 1a), the absorption parallel to the magnetic field direction increases gradually due to the alignment of the aggregates. Since the molecules orient with their long axes, that is, the dipole moment, parallel to the field, the parallel absorption increases until it saturates at a value of 3, when the alignment is complete. This maximum value is given by the maximum absorbance ratio between a randomly oriented and a fully aligned solution (integration of $\cos^2\theta$ over all angles gives $A_{\parallel} = 3A_0$). At the same time the absorbance perpendicular to the field decreases to zero with the field (Figure 1a). A completely aligned solution only absorbs light polarized parallel to the field and leaves perpendicularly polarized light unaffected.

The opposite behavior is found for molecules that align perpendicular to the field. For completely aligned solutions all molecules are oriented with the optical dipole moment perpendicular to the field, leading to an enhanced absorbance perpendicular to the field and a parallel absorbance that reduces to zero (Figure 1b). Note that the maximum value of the normalized perpendicular absorbance is limited to 1.5, and is smaller than the maximum value found for molecules that align parallel to $\vec{B}$. This reduced value is caused by the fact that, although all molecules are perfectly aligned perpendicularly to the field, they still can rotate freely about the field axis (*z*-axis) in the *xy*-plane. Since the absorption is zero when $\vec{\mu}$ is along the propagation direction of the incident light ($\phi = 90°$), this leads to a maximum value of only 1.5.

It should be noticed that these examples correspond to the two simplest situations and apply only to aggregates with a very simple arrangement in which all molecules are pointing in the same direction, such as brickwork, ladder or staircase structures. In those cases the field dependence of the absorbance together with the spectral shift of the aggregate peak (J- or H-aggregate) defines the actual molecular arrangement. More elaborate molecular architectures, such as a herringbone structure, in which not all molecules point in the same direction, will show more complicated behavior, as it combines the effect of the magnetic field on all the molecules inside.

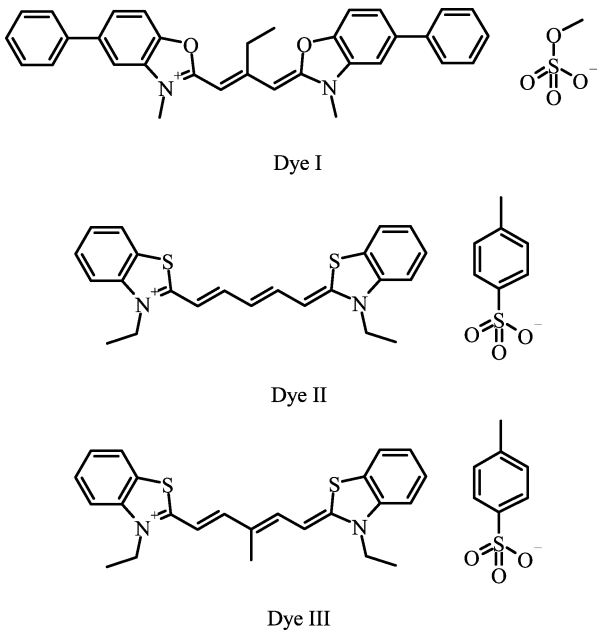

Figure 2. Structural formulas of the investigated cyanine dyes.

Furthermore, the examples are calculated using 10^5 stacked molecules, when the number of molecules is sufficiently large to cause saturation of the normalized absorbance at high fields (Figure 1) indicating complete alignment. For smaller aggregates, the alignment will not be complete, but will show a quadratic increase with field,[24] which however still can be used to determine the orientation of the molecules with respect to the field. We estimate that the field alignment of aggregates as small as 1000 molecules can be measured, well below the detection limit of X-ray and neutron diffraction.

III. Experiment

We investigated three cyanine dyes with the structural formulas shown in Figure 2, which were all synthesized by Agfa-Gevaert N. V.: 3-methyl-5-phenyl-2-[3-(3-methyl-5-phenyl-3*H*-benzoxazol-2-ylidene)-2-ethyl-1-propenyl]benzoxazolium methyl sulfate (dye I), 3-ethyl-2-[5-(3-ethyl-3*H*-benzothiazol-2-ylidene)penta-1,3-dienyl]benzothiazolium *p*-toluenesulfonate (dye II), and 3-ethyl-2-[5-(3-ethyl-3*H*-benzothiazol-2-ylidene)-3-methylpenta-1,3-di-enyl]benzothiazolium *p*-toluenesulfonate (dye III), with molecular weights 596.71, 562.78, and 576.81, respectively. Monomer solutions of different concentrations (up to 2 g/L) were prepared by dissolving dye powder in methanol. Aggregate solutions were obtained by mixing the monomer solutions with double distilled water in 1:8 proportion. For dyes II and III 0.1 M NaCl was added. Polarized absorption measurements were performed in magnetic fields up to 20 T. An optical glass cell containing the aggregate solution was mounted inside a 20 T Bitter magnet. Unpolarized light from a halogen light source was guided to the sample through an optical fiber. The light transmitted through the sample was passed through a polarizer (positioned outside the magnet) and was collected by a second fiber that coupled the light into a spectrometer containing a grating and a diode array (resolution 0.5 nm). The temperature of the sample was varied in the range 10−60 °C using a water-based temperature controller. The

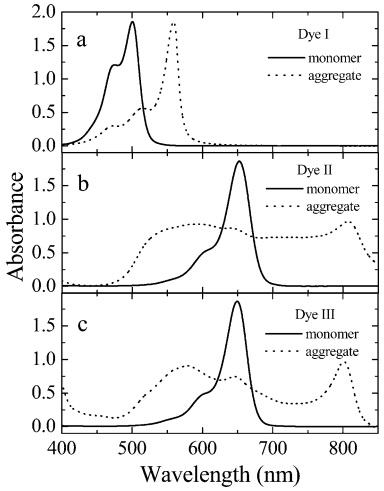

Figure 3. Absorbance spectra of monomer (solid lines) and aggregate (dashed lines) solutions of the three different dyes I (a), II (b), and III (c). Temperature = 20 °C, concentration = 1 g/L.

absorption spectra were measured for two polarizations: parallel and perpendicular to the field direction.

Single crystals were grown from methanol solution as well as from methanol−water combinations up to 1:8 proportions. To obtain large crystals, saturated solutions at 60 °C were cooled in a temperature-controlled closed cell. By lowering the temperature the solubility decreases and nucleation starts. As soon as nucleation was observed with the use of optical microscopy the temperature was raised by 2 °C to restrict the number of nucleation centers and end up with sufficiently large crystals. After a few days the crystals were collected and dried at room temperature in air. The quality of the crystals was examined by analyzing the extinction using a polarization microscope. The size and shape of the crystals were also determined. The angles between the crystal facets were measured using an optical goniometer. Crystals of high quality and good size were selected for single-crystal X-ray diffraction. Single-crystal X-ray diffraction experiments were performed using a Bruker SMART 6000 detector and Cu Kα at 100 K for dye I, a MarResearch Imaging Plate and Mo Kα at 294 K for dye II, and a Siemens P4-PC and Mo Kα at 289 K for dye III.

To obtain powder XRD diagrams of the aggregates, the aggregate solutions were filtered using 0.22 μm Millipore filters. The powder XRD diagrams were measured using a Philips PW 1820 diffractometer with a Cu target (λ = 1.5406 Å).

IV. Results

A. Polarized Absorbance. Typical absorption spectra of monomer and aggregate solutions of the studied dyes are shown in Figure 3. The monomer spectrum of dye I in methanol (Figure 3a, solid line) consists of the monomer peak at ∼500 nm and a vibronical sideband at ∼470 nm. The spectrum of dye I aggregates (Figure 3a, dashed line) reveals a narrow, intense J-band at ∼555 nm and a smaller peak at ∼510 nm, originating from the exciton coupled monomer and vibronical sideband peaks, respectively. In contrast to the appearance of a narrow, red-shifted peak upon aggregation of dye I, the aggregate solutions of dyes II and III reveal entirely different behavior (Figure 3b,c). The absorbance spectra of the aggregate solutions of these dyes show a very broad band, extending from 500 to 850 nm, with a red-shifted peak around 800 nm, a blue-shifted peak around 550 nm, and a small peak around 650 nm, probably a remaining trace of the monomer peak.

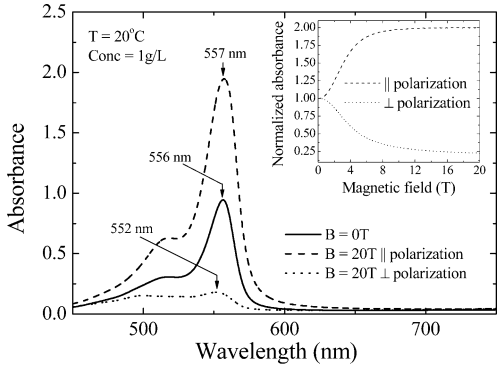

Figure 4. Absorbance spectra of the aggregate solution of dye I at 0 T (solid line) and at 20 T in parallel (dashed line) and perpendicular polarizations (dotted line). Arrows indicate the peak wavelength. Inset: changes of the J-band normalized absorbance with magnetic field for both polarizations.

All aggregate solutions show strong temperature dependence (not shown).[25] Upon heating the intensity of the aggregate peak decreases while the monomer peak becomes more pronounced, indicating that the aggregates dissolve with increasing temperature. At higher temperatures (60−70 °C depending on the concentration) the solution consists only of monomers. Subsequent cooling of the solution leads to the reappearance of the aggregate peaks in the spectrum, demonstrating that the aggregation process is thermally reversible, and that the solution contains both monomers and aggregates.

In a magnetic field the absorption spectra of the aggregate solutions become strongly polarized. The absorbance of the aggregate solution of dye I parallel to the magnetic field direction increases with the field, whereas it diminishes in the perpendicular direction (Figure 4). The effect is largest for the aggregate peak around 555 nm, of which the field-dependent normalized absorbance ($A(B)/A(0)$) is plotted in the inset of Figure 4. Note that both curves in the inset tend to saturate at fields above 10 T, indicating almost complete alignment of the J-aggregates. As the optical transition dipole moment of the dye chromophore is parallel to the line connecting both nitrogen atoms (see Figure 2), we can conclude that the aggregates orient with the long axes of the constituent molecules parallel to the magnetic field direction. Furthermore, it is important to notice that upon orientation the position of the J-peak is shifting to the red (557 nm) in the polarization parallel to the magnetic field and to the blue (552 nm) in the opposite polarization (Figure 4).

By contrast, in the case of dyes II and III, absorbance parallel to the magnetic field decreases with field, while the perpendicular absorbance increases (Figures 5 and 6). The changes are most pronounced for both red- and blue-shifted aggregate peaks, as can be most clearly seen in the results of dye III (Figure 6). For both dyes II and III the changes in absorbance do not only differ in polarization, but are also much smaller in size as compared to dye I (Figure 4), which is also evident from the field-dependent normalized absorbance curves (insets of Figures 5 and 6). As will be shown below, these effects are directly related to the molecular arrangement within the dyes, which cause the aggregates of dyes II and III to align in such a way that the dye molecules are oriented on average with their chromophores perpendicular to the magnetic field.

B. Crystal Growth and X-ray Diffraction Results. The maximum size of the obtained single crystals was found to be 1 mm for crystals grown from pure methanol in a temperature-controlled closed cell. Both the size and number of crystals strongly depend on the amount of water in the solution. More

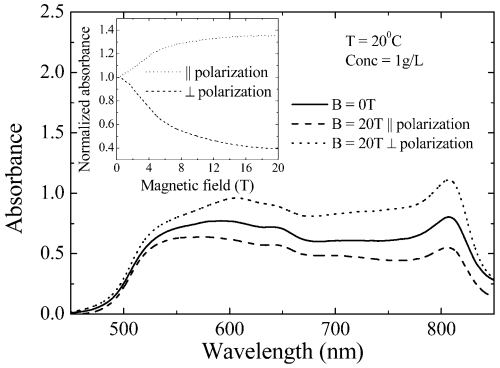

Figure 5. Absorbance spectra of the aggregate solution of dye II at 0 T (solid line) and at 20 T in parallel (dashed line) and perpendicular polarizations (dotted line). Inset: changes of the J-band absorption intensity with magnetic field for both polarizations.

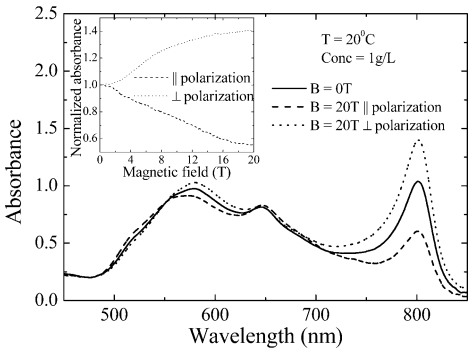

Figure 6. Absorbance spectra of the aggregate solution of dye III at 0 T (solid line) and at 20 T in parallel (dashed line) and perpendicular polarizations (dotted line). Inset: changes of the J-band absorption intensity with magnetic field for both polarizations.

TABLE 1: Crystallographic Data of the Studied Dye Single Crystals Determined from X-ray Experiments[a]

	dye I	dye II	dye III
space group	$P2_12_12_1$	Pn	$P2_1/c$
a (Å)	11.018(1)	11.274(2)	17.879(5)
b (Å)	21.445(1)	6.503(1)	7.695(2)
c (Å)	26.221(1)	21.07(4)	24.087(7)
β (deg)	90	103.07(3)	108.48(2)
Z	8	2	4
CCDC[27] code	227131	227132	227133

[a] The corresponding aggregates have the same crystal structure as judged from the powder XRD diagrams.

water resulted in more, but smaller crystals, which is explained by the fact that the dyes are hardly soluble in pure water, which can be regarded as an antisolvent. The crystals grown from pure methanol or 1:1 methanol−water solutions were observed to be nicely faceted. For each dye, judging from the crystal morphology and the XRD diagrams, no polymorphism was observed. Crystals grown from solutions containing larger amounts of water still exhibited the characteristic, albeit slightly rounded, elongated crystal shape.

Table 1 and Figure 7 summarize the crystal structures of all dyes, resulting from the extensive XRD analysis. It is important to note that comparison of the XRD data on the single crystals and the powder XRD data on the aggregates reveals that for all dyes the molecular structures of the aggregates and single crystals are the same. The crystal structure of dye I has an orthorhombic unit cell with eight molecules (space group $P2_12_12_1$, CCDC[27] code 227131), in a twisted brickwork structure (Figure 7a). The N−N axes of the molecules are aligned in the *c*-direction, and the planes of the molecules are perpendicular

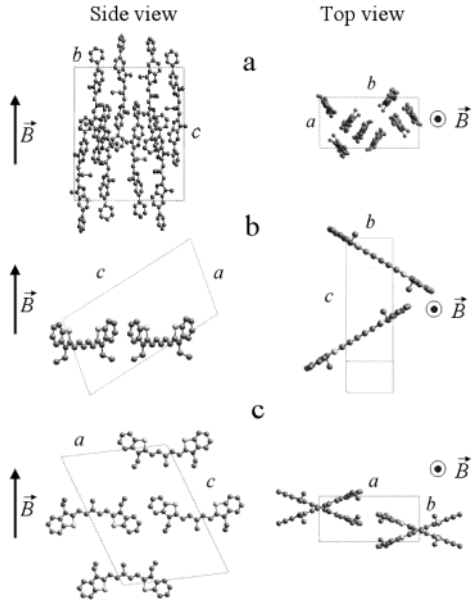

Figure 7. Crystal structures of the different dyes and their orientations in an applied magnetic field. The brickwork crystal of dye I (a) aligns along the field. The herringbone structure of dye II (b) and brickwork−herringbone structure of dye III (c) align with the long molecular axis perpendicular to the field. Counterions and solvent molecules are omitted from the cell packing for clarity.

to each other in the *ab*-plane. Dye II crystallizes in a typical herringbone structure, with a monoclinic unit cell containing two molecules (space group *Pn*, CCDC[27] code 227132) (Figure 7b). Crystals from dye III have a monoclinic unit cell consisting of four molecules (space group $P2_1/c$, CCDC[27] code 227133). Within one layer the molecules form a brickwork arrangement whereas adjacent layers form a herringbone type of structure (Figure 7c).

V. Discussion

A. Dye I. For aggregates of dye I (1 g/L, 20 °C), the normalized absorbance parallel to the magnetic field increases considerably ($A_\parallel/A_0 = 2$ at 20 T), whereas the perpendicular normalized absorbance decreases ($A_\perp/A_0 = 0.25$ at 20 T). The resulting high dichroic ratio ($A_\parallel/A_\perp = 8$) shows that (i) the aggregates have a well-defined internal ordering and (ii) the cyanine molecules are aligned with their long axis parallel to the field, resembling the situation sketched in Figure 1a. Furthermore, the intense, red-shifted, narrow absorption peak suggests a brickwork type of stacking within the aggregate.[17] Indeed, the twisted brickwork structure found for dye I necessarily leads to alignment parallel to the field. Only in this case are all aromatic rings directed parallel to the magnetic field, as indicated in Figure 7a, which is a prerequisite for minimizing the magnetic energy (section IIA). All other orientations, such as the one with the long molecular axes perpendicular to the field, always lead to a finite angle between aromatic rings and the field axis, resulting in a higher magnetic energy.

All experimental results are therefore consistent with the brickwork type of aggregates of dye I that align parallel to a magnetic field. Nevertheless, the ideal case depicted in Figure 1a, where complete parallel alignment results in an infinite dichroic ratio (because $A_\perp/A_0$ goes to zero), is not reached, which can be attributed to a number of reasons. First, increasing the concentration or decreasing the temperature, when the average size of the aggregates becomes larger, can enhance the maximum dichroic ratio significantly.[25] The magnetic field

alignment process of an aggregate strongly depends on its size (section IIA); i.e., the larger the aggregate the easier it is to align it. Since the solution consists of a distribution of aggregates with different sizes, the final dichroic ratio depends on the average aggregate size, which can be tuned by concentration and temperature.

Second, the effects of scattering and reflection of the light by the aggregates are neglected in the present analysis and will lead to small deviations from the ideal behavior. Finally, our analysis assumes that the optical response of an aggregate is governed by one chromophore, for dye I around 556 nm, oriented along the long molecular axis. In view of this it is very striking that the measured absorbance peak for perpendicular polarization (552 nm) is clearly shifted with respect to the zero field peak (556 nm), a behavior that cannot be explained by our simple model. To investigate this behavior, we have calculated the optical transition dipole moment of the actual twisted brickwork arrangement of this dye, using ZINDO semiempirical calculations.[28] This calculation reproduces the strong transition dipole moment (13.43 D) along the long molecular axis (*c*-axis) at 551 nm, close to the experimental value of 556 nm. Furthermore, an additional weaker dipole moment (0.13 D) is found, polarized along the *b*-axis, at 543 nm, 8 nm below the main transition. The experimentally observed shift can therefore be explained as follows. At the maximum magnetic field the contribution of the main aggregate peak to the perpendicular absorbance is strongly reduced, which enables the observation of the weaker, oppositely polarized absorption peak at a slightly lower wavelength. This observation further confirms the twisted brickwork arrangement of the aggregates and the usefulness of our magnetic field alignment technique, although the presence of the oppositely polarized absorption peak limits the maximum dichroic ratio that can be obtained.

B. Dyes II and III. Dyes II and III exhibit the opposite polarization behavior in magnetic field, as compared to dye I, and resemble the situation displayed in Figure 1b, with the molecules perpendicular to the field. This different alignment behavior is caused by the difference in stacking geometry. Both dyes have a herringbone structure, which implies that, in order to align all aromatic rings along the field, the aggregates orient themselves in such a way that all constituent molecules are perpendicular to the field, as is displayed in Figure 7b,c. A herringbone structure is also consistent with the appearance of two (blue- and red-shifted) absorption bands upon aggregation, as a result of the Davydov splitting.[29] Both absorption peaks behave similarly in a magnetic field and decrease (increase) simultaneously in parallel (perpendicular) polarization. Both dipole moments lie in the same plane, perpendicular to the magnetic field direction in accordance with the proposed internal structure. It should be noted, however, that our method of magnetic field alignment predicts a similar internal structure for dyes II and III. Both dyes indeed have a herringbone arrangement, but the more complicated combined brickwork−herringbone structure of dye III cannot be distinguished from the herringbone structure of dye II.

VI. Conclusions

We have presented a new technique to determine the internal structure of dye aggregates in solution by measuring the polarized absorbance spectra of magnetically aligned aggregates. We have demonstrated our method by using three different cyanine dyes, each with a different molecular arrangement, which are essentially identical to the crystal structures obtained by single-crystal X-ray diffraction experiments. The applicability of our technique is not restricted to cyanine dyes, but our method can also be used for novel functional materials, such as thiophenes, phenylenevinylenes, and perylenes, which are promising for the development of new optical and electrical (thin-film) devices, provided the self-organization of these molecules into well-defined assemblies can be controlled.

References and Notes

(1) Braun, E.; Eichen, Y.; Sivan, U.; Ben-Yoseph, G. *Nature* **1998**, *391*, 775.

(2) McDermott, G.; Prince, S. M.; Freer, A. A.; Hawthornwaitelawless, A. M.; Papiz, M. Z.; Cogdell, R. J.; Isaacs, N. W. *Nature* **1995**, *374*, 517.

(3) Schenning, A. P. H. J.; Jonkheijm, P.; Peeters, E.; Meijer, E. W. *J. Am. Chem. Soc.* **2001**, *123*, 409.

(4) Bumm, L. A.; Arnold, J. J.; Cygan, M. T.; Dunbar, T. D.; Burgin, T. P.; Jones, L.; Allara, D. L.; Tour, J. M.; Weiss, P. S. *Science* **1996**, *271*, 1705.

(5) Biemans, H. A. M.; Rowan, A. E.; Verhoeven, A.; Vanoppen, P.; Latterini, L.; Foekema, J.; Schenning, A. P. H. J.; Meijer, E. W.; de Schrijver, F. C.; Nolte, R. J. M. *J. Am. Chem. Soc.* **1998**, *120*, 11054.

(6) Kato, N.; Saito, K.; Aida, H.; Uesu, Y. *Chem. Phys. Lett.* **1999**, *312*, 115.

(7) Vacha, M.; Saeki, M.; Furuki, M.; Pu, L. S.; Hashizume, K.; Tani, T. *J. Lumin.* **2002**, *98*, 35.

(8) Janssens, G.; Touhari, F.; Gerritsen, J. W.; van Kempen, H.; Callant, P.; Deroover, G.; Vandenbroucke, D. *Chem. Phys. Lett.* **2001**, *344*, 1.

(9) Vacha, M.; Takei, S.; Hashizume, K.; Sakakibara, Y.; Tani, T. *Chem. Phys. Lett.* **2000**, *331*, 387.

(10) Yoshikawa, H.; Masuhara, H. *J. Photochem. Photobiol. C: Photochem. Rev.* **2000**, *1*, 57.

(11) von Berlepsch, H.; Bottcher, C.; Ouart, A.; Burger, C.; Dahne, S.; Kirstein, S. *J. Phys. Chem. B* **2000**, *104*, 5255.

(12) Sturmer, D. M.; Heseltine, D. W. In *Theory of Photographic Process*, 4th ed.; James, T. H., Ed.; Macmillan: London, 1977.

(13) Dougherty, T. J.; Kaufman, J. E.; Goldfarb, A.; Weishaupt, K. R.; Boyle, D. G.; Mittelman, M. *Cancer. Res.* **1978**, *38*, 2628.

(14) Maeda, M. *Laser Dyes*; Academic: Tokyo, 1984.

(15) Spano, F. C.; Mukamel, S. *Phys. Rev. Lett.* **1991**, *66*, 1197.

(16) Knoester, J. *Phys. Rev. A* **1993**, *47*, 2083.

(17) Kobayashi, T. *J-aggregates*; World Scientific Publishing Co: Singapore, 1996.

(18) Jelly, E. E. *Nature (London)* **1936**, *138*, 1009.

(19) Scheibe, G. *Angew. Chem.* **1936**, *49*, 536.

(20) Brooker, L. G. S.; White, F. L.; Heseltine, D. W.; Keyes, G. H.; Dent, S. G.; van Lare, E. J. *J. Photogr. Sci.* **1953**, *1*, 173.

(21) Harrison, W. J.; Mateer, D. L.; Tiddy, G. J. *J. Phys. Chem.* **1996**, *100*, 2310.

(22) Czikkely, C.; Forsterling, H.; Kuhn, H. *Chem. Phys. Lett.* **1970**, *6*, 207.

(23) de Gennes, P. G.; Prost, J. *Physics of Liquid Crystals*; Clarendon Press: Oxford, 1993; p 118.

(24) Maret, G.; Dransfeld, K. In *Strong and Ultrastrong Magnetic Fields and Their Applications*; Springer-Verlag: Berlin, 1985; Chapter 4 and refs therein.

(25) Shklyarevskiy, I. O.; Boamfa, M. I.; Christianen, P. C. M.; Touhari, F.; van Kempen, H.; Deroover, G.; Callant, P.; Maan, J. C. *J. Chem. Phys.* **2002**, *116*, 8409.

(26) Ward, I. M. Determination of Molecular Orientation by Spectroscopic Techniques. In *Advances in Polymer Science*; Springer-Verlag: Berlin, 1985; Vol. 66, p 81.

(27) Cambridge Crystallographic Data Center (CCDC) home page: http://www.ccdc.cam.ac.uk.

(28) Zutterman, F.; Deroover, G.; Callant, P. Unpublished results.

(29) Davydov, A. S. *Theory of molecular excitons*; Plenum Press: New York, 1971.